Mon. Not. R. Astron. Soc. **280,** 235–251 (1996)

Autofib Redshift Survey – I. Evolution of the galaxy luminosity function

Richard S. Ellis,[1] Matthew Colless,[2] Tom Broadhurst,[3] Jeremy Heyl[1,4] and Karl Glazebrook[1]

[1]*Institute of Astronomy, Madingley Road, Cambridge CB3 0HA*
[2]*Mount Stromlo and Siding Spring Observatories, The Australian National University, Weston Creek, ACT 2611, Australia*
[3]*Department of Physics and Astronomy, Johns Hopkins University, Baltimore MD 21218, USA*
[4]*Lick Observatory, Board of Studies in Astronomy and Astrophysics, University of California, Santa Cruz, CA 95064, USA*

Accepted 1995 November 23. Received 1995 November 21; in original form 1995 August 22

ABSTRACT

We present a detailed determination of the rest frame B-band galaxy luminosity function (LF) as a function of redshift and star formation activity from $z=0$ to $z\simeq 0.75$. The data set used for this purpose is a composite sample of over 1700 redshifts spanning a wide range in apparent magnitude, $11.5<b_{\rm J}<24.0$, which we term the Autofib Redshift Survey. The sample includes various earlier magnitude-limited surveys constructed by our team, as well as a new survey of 1026 redshifts measured for galaxies at intermediate magnitudes. Spectral classifications, essential for estimating the k-corrections and galaxy luminosities, are accomplished via cross-correlation with Kennicutt's library of integrated galaxy spectra. The various overlapping surveys in the sample enable us to assess the effects of redshift incompleteness. We demonstrate that uncertainties in classification and those arising from incompleteness do not seriously affect our conclusions.

The large range in apparent magnitude sampled allows us to investigate both the nature of the LF at low redshifts ($z<0.1$) and the possible evolution in its shape to $z=0.75$. We find that earlier bright surveys have underestimated the absolute normalization of the LF. Because the shape of the local LF does not change with the apparent-magnitude limit of the survey, it seems unlikely that the local deficiency arises from an underestimated population of low-luminosity galaxies. Furthermore, surface-brightness losses cannot be significant unless they conspire to retain the LF shape over a variety of detection thresholds.

Our data directly demonstrate that the B-band LF evolves with redshift. This evolution is best represented as a steepening of the faint-end slope of the LF, from $\alpha\simeq -1.1$ at low redshift to $\alpha\simeq -1.5$ at $z\simeq 0.5$. Using [O II] emission as an indicator of star-formation activity, we show that the LF of quiescent galaxies has remained largely unchanged since $z\simeq 0.5$, whereas the luminosity density of star-forming galaxies has declined by more than 50 per cent. The steepening of the overall LF with look-back time is of the form originally postulated by Broadhurst, Ellis & Shanks and is a direct consequence of the increasing space density of blue star-forming galaxies at moderate redshifts.

Key words: galaxies: evolution – galaxies: luminosity function, mass function – cosmology: observations – large-scale structure of Universe.

1 INTRODUCTION

The detailed characterization of the luminosity function (LF) of field galaxies is an important extragalactic question. Notwithstanding several controlled redshift surveys of field galaxies in recent years (Kirshner, Oemler & Schechter 1978; Peterson et al. 1985; Loveday et al. 1992), some uncertainty clearly remains in both the absolute normalization of the LF, ϕ^* (see Maddox et al. 1990), and the faint-end slope, α (Davies 1990; McGaugh 1994). A further important issue is the nature of any dependences of these quantities on morphological type. A steep faint-end slope of the LF is a

natural consequence of hierarchical models of galaxy formation seeded at early times by cold dark haloes (Lacey et al. 1992; Kauffmann, Guiderdoni & White 1994; Cole et al. 1994). Improved observational constraints on these models are required.

Our present knowledge of the field galaxy LF comes primarily from redshift surveys limited at $B \approx 17$. Although some of these samples (such as the Stromlo–APM and CfA surveys) are extensive, they are not optimally designed to address issues concerning the faint-end slope, α. Their main value has been in defining very precisely the value of M^*, verifying that the Schechter (1976) formula is an appropriate representation, and providing limited constraints on the form of the LF for $M_B < -13 + 5 \log h$ (where h is Hubble's constant in units of 100 km s^{-1} Mpc^{-1}). At $B \approx 17$, a dwarf galaxy with $M_B = -14 + 5 \log h$ can barely be detected beyond the Virgo cluster. Even in panoramic surveys, the volumes probed to this apparent-magnitude limit are insufficient to constrain the abundance of such dwarf galaxies. Small local volumes may also be unrepresentative. A further problem with intermediate-depth surveys is that the photometric data on which many are based either are not well defined or are insufficiently deep in their surface-brightness limit to reveal possible low-surface-brightness systems which may dominate the faint end of the LF (McGaugh 1994; Ferguson & McGaugh 1995).

The contribution of dwarf galaxies may be crucial to understanding analyses of deeper ($B > 21$) surveys of cosmological importance and, in particular, in quantifying the nature of any faint excess in the galaxy counts (Ellis 1993). Even a minor change in α can produce a dramatic increase in the expected number of $B > 21$ galaxies, since galaxies at the faint end of the LF contribute to the number counts with a steep Euclidean slope (Kron 1980; Phillipps & Driver 1995). A related issue here is the normalization of the local LF. Galaxy counts at intermediate magnitudes $17 < B < 21$ (Heydon-Dumbleton, Collins & MacGillivray 1989, Maddox et al. 1990) present a puzzlingly steep slope. If these data are correct and evolution at such bright magnitudes is discounted, ϕ^* may not be well determined. An upward revision by a factor of 2 would reduce the faint excess brighter than $B \approx 21$–22 and explain photometric colour and redshift distributions which both match no-evolution expectations (Metcalfe et al. 1995a).

Although one motivation for deeper spectroscopic surveys is the need to clarify these uncertainties in the local LF, the main goal of the fainter surveys carried out to date has been to search for evolution in the LF (see Koo & Kron 1992 and Ellis 1993 for a review of these efforts). Spectroscopic surveys consisting of 100–300 galaxies in strict magnitude-limited samples fainter than $B = 21$ have been published by Broadhurst, Ellis & Shanks (1988, hereafter BES), Colless et al. (1990, 1993), Lilly, Cowie & Gardner (1991), Lilly et al. (1995) and Cowie, Songaila & Hu (1991). A consistent picture has emerged from these surveys. Notwithstanding the apparent excess of faint galaxies, the redshift distributions reveal no unexpected high- or low-redshift tails. To first order, the $N(z)$ distribution results are compatible with evolution in galaxy number density, rather than in the luminosity scale. BES claim a rising fraction of star-forming galaxies displaying intense [O II] emission but the validity of this result, the only direct evidence for evolution in the population, relies on accounting for the various aperture and k-correction biases (see Koo, Gronwall & Bruzual 1993).

For reasons of observing efficiency, the deep spectral surveys consist of samples restricted to lie within narrow apparent-magnitude ranges. This precludes any *direct* estimation of the LF as a function of redshift. For example, although BES were able to demonstrate that the redshift distribution of their faint survey was consistent with an LF whose faint-end slope steepens with increasing redshift (see their fig. 8), they were not able to observe such steepening directly in their data. The effect proposed by BES would produce an effective increase in the number density of luminous galaxies at approximately M^* (and hence in the excess counts) *without* distorting the redshift distribution from its no-evolution expectation. Eales (1993) attempted to combine the various surveys to derive a direct estimate of the LF as a function of redshift; however, the inhomogeneity and limited size of the data sets then available precluded very reliable conclusions.

In this series of papers we present the results of a comprehensive new survey, the Autofib Redshift Survey, conducted with AAT's Autofib fibre positioner (Parry & Sharples 1988). The primary role of the new data is to fill a 'gap' in the coverage of apparent magnitudes in the range $B = 17$–21 and to increase significantly the size of the sample out to $B = 22$.

The scientific motivation of the survey is two-fold. First, by extending the local surveys to fainter limits, more rigorous constraints can be provided on the faint-end slope and normalization of the local LF. Secondly, with strategically constructed samples spanning a wide apparent-magnitude range, we can monitor directly, for the first time, any evolution in the form of the LF with redshift. With a large enough sample it is also possible to check for evolution as a function of spectral class.

Galaxy selection in the B photometric band is advantageous for this large survey not only because it makes optimal use of existing data, but also because it maximizes the sensitivity to recent changes in the global star formation rate of galaxies of various kinds. Our survey is able to address directly the long-standing question of the origin of the excess number of B-band galaxies. It complements recent work in the I band (Lilly 1993; Lilly et al. 1995) and in the K band (Cowie 1993; Glazebrook et al. 1995b), whose role is equally important in clarifying longer-term changes in galaxy properties over slightly larger redshift baselines.

This first paper in the series presents the main scientific conclusions of the survey. In Paper II (Heyl et al. 1996) we discuss in more detail the luminosity function of various spectral classes as a function of redshift. Paper III (Broadhurst et al. 1996) discusses the observing strategy and presents the redshift survey catalogue and related quantities for over 1700 galaxies.

The plan of this paper is as follows. In Section 2 we briefly summarize our overall strategy, the incorporation of data from previous surveys, and the new observations conducted with Autofib. In Section 3 we discuss the analysis of the data, including a technique developed to derive k-corrections for individual galaxies based on a classification of their spectra, and a simple estimator for deriving the luminosity function in different redshift bins. Section 4

presents the results, including new constraints on the local LF and evidence for evolution in the form of the LF with redshift for the entire sample and for various spectral subclasses. Section 5 discusses the conclusions of the survey in the context of various explanations proposed for the demise of the faint blue galaxy population.

2 THE AUTOFIB REDSHIFT SURVEY

2.1 Strategy

The principal goal of the new Autofib survey is to extend the range of galaxy luminosities sampled at moderate redshift by sampling the apparent-magnitude–redshift plane between the early $B<17$ surveys and the more recent $20<B<24$ surveys. With this broad coverage of apparent magnitude, *direct* estimates of the luminosity function (LF) at various redshifts can be obtained. A detailed account of our observing strategy and sample selection will be given in Paper III. Here we briefly summarize the salient points.

The new data consist of 1028 redshifts in 32 pencil beams within two apparent-magnitude ranges: $17<b_J<20$ (AF-bright) and $19.5<b_J<22$ (AF-faint). By sampling many different directions rather than a single contiguous area the confusing effects that galaxy clustering may have on the derived LFs can be minimized. The different sampling rates for the various magnitude ranges enable us to make effective use of a limited amount of observing time and to populate the apparent-magnitude–redshift plane in a well-controlled way.

Table 1 summarizes the overall survey characteristics. As well as the new data, we have included the brighter DARS survey (Peterson et al. 1985) and the fainter surveys of BES, LDSS-1 (Colless et al. 1990, 1993) and LDSS-2 (Glazebrook et al. 1995a). In total, our catalogue contains 1701 galaxy redshifts and three QSOs. The galaxies have redshifts up to $z=1.108$; the QSOs have $z=1.262$, 1.493 and 1.599. The composite survey consists of 53 pencil beams and spans the apparent-magnitude range $b_J=11.5$–24.0. The large number of pencil beams spans many widely separated fields over the entire southern sky, and thus a very large volume is effectively randomly sampled. Paper III in this series (Broadhurst et al., in preparation) presents the composite survey catalogue and a field-by-field summary of the selection criteria, sampling rate and redshift completeness.

Details of the photometric selection, observing techniques and spectroscopic analyses for the published data can be found in the relevant references or in Paper III. All galaxy photometry has been reduced to the colour-corrected photographic $b_J \equiv$ Kodak IIIa-J plus GG395 at a limiting surface brightness of $\mu_J=26.5$ mag arcsec^{-2} (Jones et al. 1991). For the new data in the intermediate range observed with Autofib, objects were selected from COSMOS measuring-machine scans of sky-limited UK Schmidt plates using a typical threshold of $\mu_J=25.0$ mag arcsec^{-2}. This photometry was calibrated with reference to $19<b_J<21$ galaxies in the APM galaxy survey (Maddox et al. 1990) in all cases where the fields overlap, and with the Edinburgh–Durham southern galaxy survey (Heydon-Dumbleton et al. 1989) for the remainder. In producing a uniform photometric catalogue, corrections were made for the different isophotes used in each catalogue (Peterson et al. 1985). These corrections are always smaller than 0.28 mag and are thus comparable to the random photometric errors, which vary from 0.05 to 0.15 mag across the catalogue.

Star/galaxy separation for the DARS and BES data was performed by eye. For the fainter LDSS-1 and LDSS-2 surveys, *all* objects were observed spectroscopically, and galaxy samples were defined from the spectra obtained. Whereas the penalty of including stars in the deep surveys is small, the additional overhead of this mode of observing at $b_J=17$–20 would be prohibitive. Previous all-inclusive surveys (Tritton & Morton 1984; Colless et al. 1990, 1991, 1993; Glazebrook et al. 1995a) have failed to find a significant extragalactic population of compact sources. In the new data reported here, we therefore relied on the COSMOS star–galaxy classification algorithm, making additional visual checks of each selected target prior to undertaking spectroscopic observations.

2.2 Incompleteness

Incompleteness can arise in several ways, and, if it were systematic with redshift or spectral type, might seriously affect LF estimation. The most benign effect, which can be corrected, is incompletenes that arises purely from the increased difficulty of making redshift identifications because the spectra of the fainter galaxies in each of the various magnitude ranges have inadequate signal-to-noise ratios. *Provided* this magnitude-dependent incompleteness is independent of redshift or type, then it can be corrected by weighting each galaxy inversely with the survey success rate at that apparent magnitude. The completeness as a function of apparent magnitude for the various surveys is shown in Fig. 1. All the surveys show some drop in completeness at the faint end of their magnitude range. The worst-affected surveys are AF-bright and LDSS-2, while DARS is virtually complete. The relatively low completeness of the AF-bright survey arises from our strategy of carrying out the observations for this survey whenever the

Table 1. The redshift surveys.

Survey	b_J	Area □°	Fields	Gals	ID%	$\langle V/V_{max}\rangle$ raw	$\langle V/V_{max}\rangle$ corr	$d\langle V/V_{max}\rangle$	n	m	n'
DARS	11.5–17.0	70.840	5	328	96%	0.46	0.46	0.016	2.5	3.5	1.3
AF-bright	17.0–20.0	5.519	16	478	70%	0.43	0.48	0.013	1.8	1.9	1.3
AF-faint	19.5–22.0	4.670	16	548	81%	0.45	0.46	0.012	3.6	1.5	2.9
BES	20.0–21.5	0.499	5	188	83%	0.44	0.47	0.021	1.4	0.8	1.4
LDSS-1	21.0–22.5	0.124	6	100	82%	0.44	0.46	0.029	1.4	1.3	1.2
LDSS-2	22.5–24.0	0.096	7	84	72%	0.48	0.52	0.038	0.5	1.6	0.4

conditions were too poor for the AF-faint survey. As a consequence, the AF-bright spectra are often of poorer quality than the AF-faint spectra.

We can estimate the effect of the observed incompleteness (and the efficacy of a magnitude-dependent completeness correction of the type described above) by comparing the distributions of the V/V_{max} statistic for the various data subsets with and without the correction for magnitude-dependent incompleteness. If the observed distribution of galaxies is inclustered and does not evolve, then V/V_{max} should be uniformly distributed between 0 and 1. Actual clustering and evolution will cause departures from this expectation, but so will magnitude-dependent incompleteness even in their absence.

The form of departure from uniformity of the V/V_{max} distribution is different for each of these cases. Magnitude-dependent incompleteness will cause the sample to be deficient in the higher redshift galaxies of any given luminosity, and will therefore bias the V/V_{max} distribution to smaller values; clustering will cause peaks and troughs in the distribution at the values of V/V_{max} corresponding roughly to an L^* galaxy at the redshift of the relevant structure; evolution (at least if it takes the form of an increase in the number of galaxies of any given luminosity at higher redshifts) will bias the distribution to larger values. Note that an important feature of our strategy of breaking our samples into several narrow apparent-magnitude slices, is that we expect little relative evolution over any one subsample. Only by combining all the surveys and spanning a large range in apparent magnitude and redshift do we expect to see evidence for evolution. Thus the absence of any upward trend within a survey covering a narrow apparent-magnitude range is not evidence against evolution.

Table 1 lists the mean value of the V/V_{max} statistic for each survey before and after applying the correction for magnitude-dependent incompleteness (which is shown as the dotted lines in Fig. 1). Uncertainties refer to standard errors in the mean of N instances of a uniform random variable,

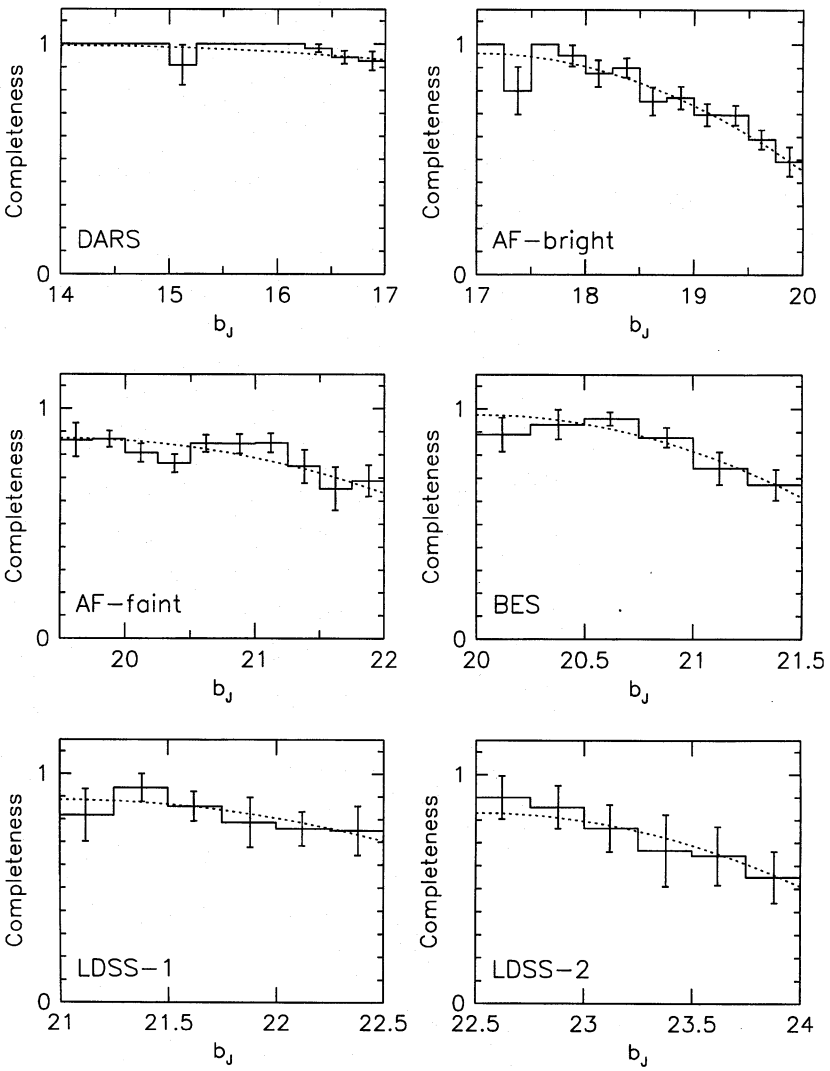

Figure 1. Completeness as a function of apparent magnitude for the various surveys. The dotted lines are the fits used in applying the magnitude-dependent completeness corrections.

viz. $\sqrt{1/12N}$. The table indicates the significance with which our observed values (after correction) depart from the expectation value of 0.5.

Clustering increases the uncertainty of this test. If there are typically m objects per cluster, the uncertainty in V/V_{max} becomes $\sqrt{m/12N}$. We can estimate m very crudely by considering the observed standard deviations s in the V/V_{max} histograms: for 10 bins, we obtain $m=10s^2/N$. With these values of m, the revised $n'=n/\sqrt{m}$ is consistently less than 3, suggesting that no significant non-uniformities remain in the completeness-corrected samples. We will demonstrate later that the effect of this remaining incompleteness on the LFs is small.

Unlike magnitude-dependent effects, incompleteness that is a function of galaxy redshift or spectral type can be neither directly quantified nor corrected. Furthermore, both these forms of incompleteness may be confused with the signal-to-noise ratio-dependent losses, since both type and redshift are expected to correlate with apparent magnitude. We can, however, conduct tests to establish whether either of these problems is significant.

For type-dependent incompleteness we can again use the V/V_{max} statistic. In Section 3.1 we define a procedure to allocate a spectral type to each galaxy by correlating its spectrum with local templates. Anticipating this classification scheme, Fig. 2 shows V/V_{max} distributions for each spectral type (as defined in Section 3.1) with and without the correction for magnitude-dependent incompleteness. In every case the correction leads to more uniform V/V_{max} distributions (i.e. $\langle V/V_{max}\rangle$ closer to 0.5), although a slight deficit of objects with large values of V/V_{max} still remains.

For redshift-dependent incompleteness, the V/V_{max} statistic is inapplicable because V is a function of z. We can, however, check for redshift-dependent incompleteness by making use of the important fact that our combined sample is made up of subsurveys with overlapping apparent-magnitude ranges. By comparing the redshift distribution of the bright (high-completeness) end of a fainter survey with the

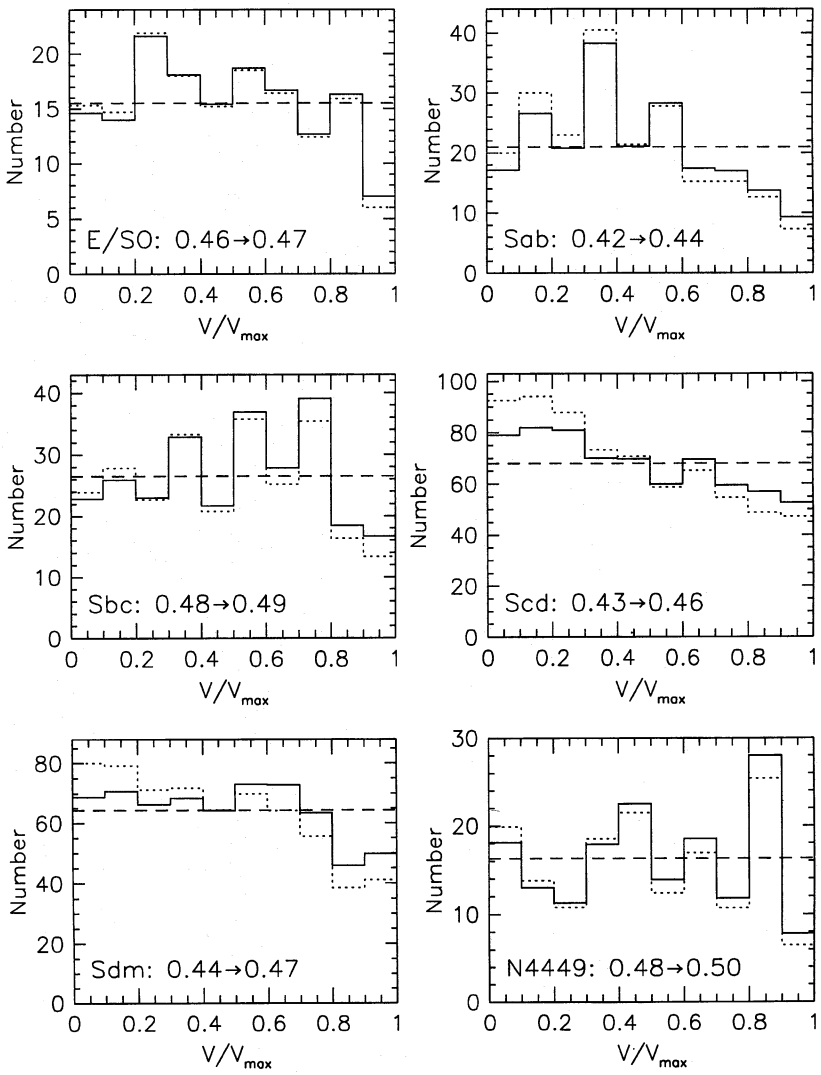

Figure 2. V/V_{max} distributions for each spectral type. The dotted lines show the distributions before applying the magnitude-dependent completeness corrections and the solid lines, after. The values of $\langle V/V_{max}\rangle$ before and after the corrections are indicted.

faint (low-completeness) end of a brighter survey we can, within the limits imposed by clustering, check whether incompleteness distorts the redshift distributions. By restricting the LF analyses to those based on data within limited redshift ranges, we can limit the effect of such incompleteness further.

Fig. 3 shows the results of such comparisons. With the exception of the overlap between AF-bright and AF-faint there is good agreement between the redshift distributions, implying that redshift-dependent incompleteness is not a problem. Of course we cannot check the LDSS-2 survey in this way since we have no fainter survey with which to compare it. Glazebrook et al. (1995a) discuss the limitations of this deepest data set in some detail. The significant difference between the AF-bright and AF-faint data in the range $b_J = 19.5–20$ is difficult to understand. It seems difficult to attribute this to redshift-dependent incompleteness, given the ranges involved ($z \simeq 0.1$ in AF-bright cf. 0.2–0.3 in AF-faint). Conceivably this is a clustering effect or arises from the small sample sizes.

To summarize, there is significant incompleteness in all the surveys included in this work. This incompleteness, however, appears to be dominated by the difficulty of identifying the fainter galaxies in each sample, due to their poorer spectral signal-to-noise ratio. We can remove this effect satisfactorily by applying a magnitude-dependent completeness correction. Although some residual systematic effects remain, these are small; we show later that even the dominant magnitude-dependent correction does not seriously affect our LF results.

3 ANALYSIS

The full Autofib survey catalogue containing positions, photometry and spectral classifications will be published in Paper III. The raw data for analysis consists of galaxy positions precise to better than 0.5 arcsec rms, b_J magnitudes and redshifts. The first and most important step in determining the galaxy LF is calculating the luminosity. Once a cosmological framework has been selected (we adopt $q_0 = 0.5$ and $H_0 = 100\,h$ km s^{-1} Mpc^{-1}), the distance modulus for each galaxy can be readily determined. In samples at moderate redshifts, however, the k-correction is a very significant term and a strong function of spectral class and redshift. For the range of Hubble types seen locally, the k-correction for the b_J system ranges from 0 to 2 mag at the

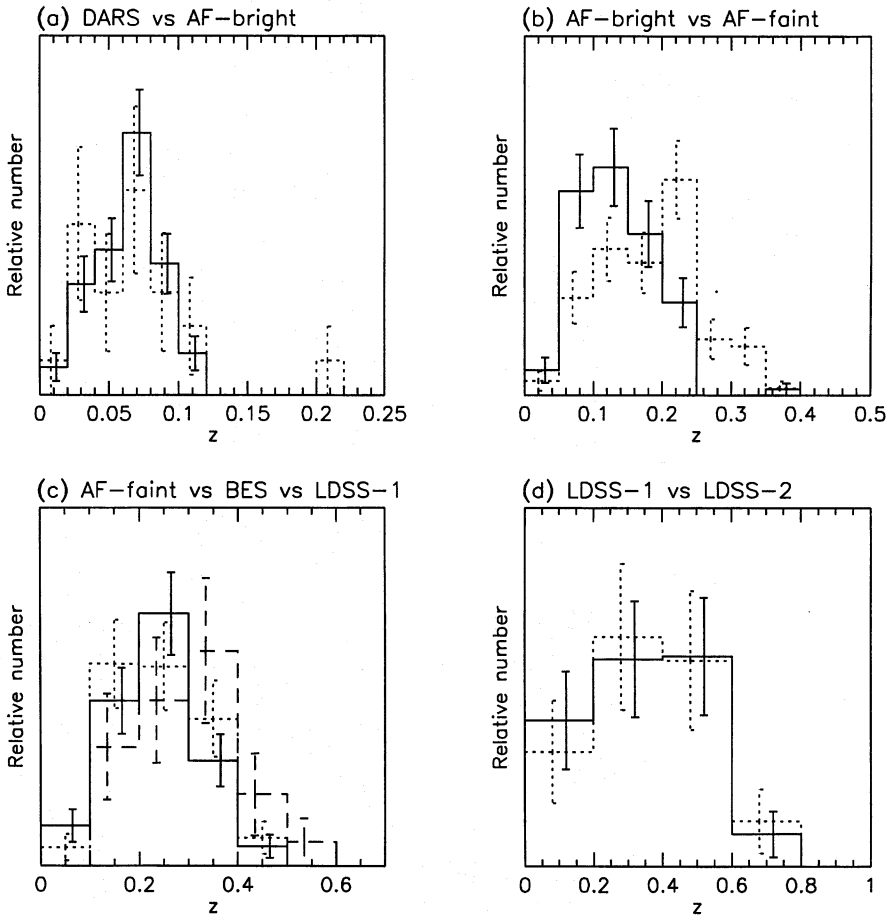

Figure 3. Comparison of the redshift distributions in the overlap magnitude ranges of the various surveys. In each panel the first survey is the solid line, the second is dotted, and the third is dashed. The distributions are normalized to have the same total number of objects. Poisson error bars are shown. (a) DARS $b_J = 16.5–17$ versus AF-bright $b_J = 17–17.5$; (b) AF-bright versus AF-faint, both in $b_J = 19.5–20$; (c) AF-faint versus BES versus LDSS-1, all with $b_J = 21–21.5$; (d) LDSS-1 $b_J = 22–22.5$ versus LDSS-2 $b_J = 22.5–23$.

mean redshift of the LDSS-2 data, and 0 to 1 mag even at the mean redshift of the AF-faint data. In order to make progress, therefore, we also need to define a robust classification procedure from which type-dependent k-corrections can be estimated for every galaxy in the survey.

3.1 *k*-corrections

Previous researchers have used a variety of approaches to estimate k-corrections. The most common method is to assume that galaxies have k-corrections that increase linearly with redshift, with each morphological type assigned a different slope (e.g. Efstathiou, Ellis & Peterson 1988; Loveday et al. 1992). If colours are available, the observed colour and redshifts can be used to infer the spectral type by comparison with predictions from a set of template spectral energy distributions, and the k-correction then follows (e.g. Colless et al. 1990). In a preliminary analysis prior to that carried out here, Eales (1993) used the alternative approach of calculating luminosities in a passband corresponding to the b_J band shifted blueward by the mean redshift of the sample. This has the advantage that errors in the k-correction are minimized, as the correction at the mean redshift is defined to be zero. Eales, however, was unable to assign types to any but the nearest galaxies in his analysis (those in DARS), and thus his luminosities could be in error by as much as 1 mag.

For the Autofib redshift survey, the above-mentioned methods for obtaining k-corrections are either inapplicable or inadequate. Only the DARS galaxies are bright enough for morphological classification, and only the LDSS-1 and LDSS-2 samples have b_J–r_F colours, while applying a mean k-correction or using a mean redshift gives large errors in the inferred luminosities and even larger errors in the volume weighting necessary to recover the LF.

The ideal solution would be to derive the k-correction directly from each spectrum. To do this we would need to sample the b_J response curve ($\lambda\lambda$3800–5400) in both the observed and the rest frames. For high-redshift objects, however, the rest frame b_J lies outside our spectral range. We would also need to have reliable flux-calibrated data, but this is difficult at faint limits, where the sky-subtraction introduces uncertainties that make the spectra adequate only for identifying features.

Clearly the way forward is to *classify* the spectra and relate this classification to a well-defined set of k-corrections. Rather than relying on specific spectral features (which may not always be present), we chose to cross-correlate the survey spectra against those of the Kennicut (1992a, b) spectral library of similar spectral resolution. These library spectra are well suited for use as cross-correlation templates because their wavelength coverage matches our survey spectra well and because they sample the integrated light of the galaxies, which is approximately also the case for our fibre and slit spectra of faint galaxies.

Prior to cross-correlation, the Kennicut template spectrum and the survey spectrum were smoothed on a 100-Å scale in the observer's frame. The smoothed versions were then subtracted, yielding continuum-subtracted spectra rebinned to 2 Å per pixel. The survey spectrum was then assigned the type of the template with which it was most strongly cross-correlated. The published morphology of the appropriate Kennicut template indicates which of the King & Ellis (1985) k-corrections was used for that particular survey spectrum. This table of k-corrections is available for E/S0, Sab, Sbc, Scd, Sdm types and for NGC 4449, the latter being an intense star-forming galaxy representative of the bluest classes identified in our survey. An illustration of this method is given in Fig. 4.

To check this algorithm, we performed a series of simulations. A Kennicut spectrum was selected at random and normalized to a suitable mean count per pixel. This spectrum was next redshifted by a random z between 0 and 0.6, multiplied by an approximation to the instrumental response function, and then brought back to zero redshift. Finally, the observed spectrum was generated as a set of random Gaussian deviates about this modified template spectrum with a signal-to-noise ratio per pixel in the range 0.8–4.0. These test spectra were processed similarly to the real survey spectra. The success rate in identifying the correct spectral type was highly satisfactory: averaging over all redshifts, the success rate was 70 per cent for spectra with a signal-to-noise ratio $=1$ per pixel and >80 per cent for spectra with a signal-to-noise ratio of >2 per pixel; averaging over all signal-to-noise ratio levels, the success rate is >80 per cent for $z<0.5$; for $z>0.5$ the success rate drops to 40 per cent, however, a consequence of the lack of overlap in the rest frame between the templates and the observed spectra.

We therefore classified the galaxy spectra from the various surveys as follows: (i) for DARS we used the morphological types given by Peterson et al. (1985); (ii) for AF-bright, AF-faint and BES we used the cross-correlation method described above; (iii) for LDSS-1 we used the cross-correlation method supplemented by the use of the published $b_J - r_F$ colours for galaxies that were either at too high a redshift or had too low a signal-to-noise ratio for the method to be reliable; (iv) for LDSS-2 we used the published $B-R$ colours to infer spectral types. For the 136 galaxies where we could not classify a spectrum with the cross-correlation method and where we did not have either a morphological type or colour, we used the k-correction appropriate to an Scd (the median spectral type of the whole survey) in computing its luminosity.

As an external check on the cross-correlation classifications, we can compare the $b_J - r_F$ colour observed for those galaxies in the LDSS-1 survey (Colless et al. 1990) with the colour predicted from the galaxy's redshift and its spectral type as derived by the cross-correlation method (see Fig. 5). The agreement is generally very good: the rms scatter of 0.4 mag reflects both the expected 0.2 mag rms uncertainties in the observed colours and a small number of objects with odd colours resulting from image mergers on the plate, as well as the errors in the spectral classifications.

A detailed description of the spectral classification algorithm and more exhaustive tests of the method are given in Paper II. We can, however, illustrate the precision attained by assuming that 20 per cent of the galaxies are misclassified by one class equally in both directions – an error consistent with the discussion in Paper II. We can then calculate the rms k-correction error for a given redshift bin and class from the differential trends with class, including an allowance for the fact that the class is a discrete approximation to the actual spectral energy distribution. The errors

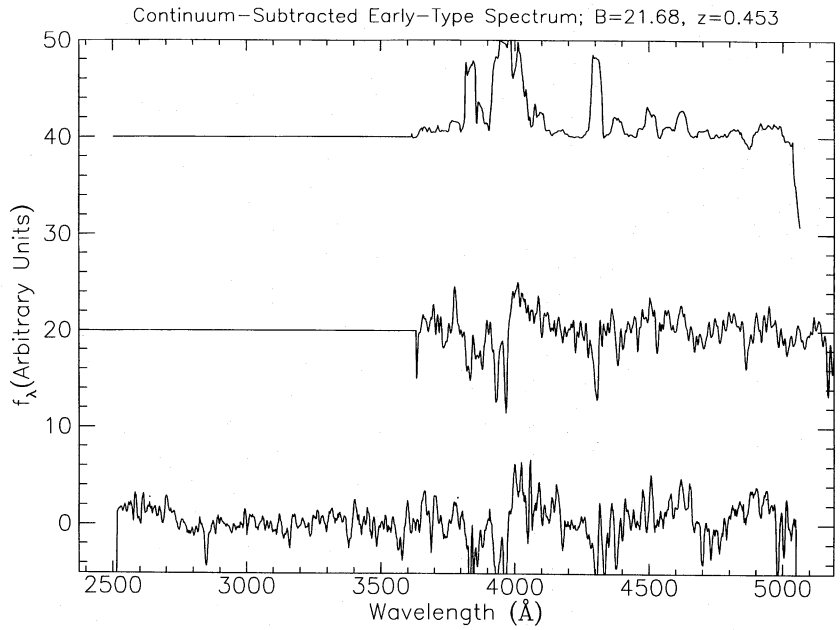

Figure 4. Example of spectral classification by the cross-correlation method. The middle curve shows the continuum-subtracted spectrum of a $z=0.453$ galaxy with $b_J=21.68$ from the AF-faint survey. The lower curve is the best-matching template spectrum from the Kennicutt atlas, which belongs to an early-type (Sab) galaxy. The upper curve shows the cross-correlation of the two spectra.

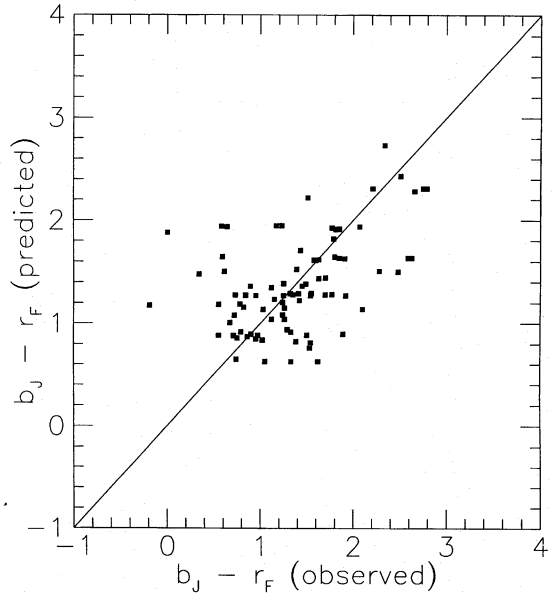

Figure 5. Comparison of the observed b_J-r_F colours of LDSS-1 survey galaxies with their colours as predicted from their redshifts and cross-correlation spectral types.

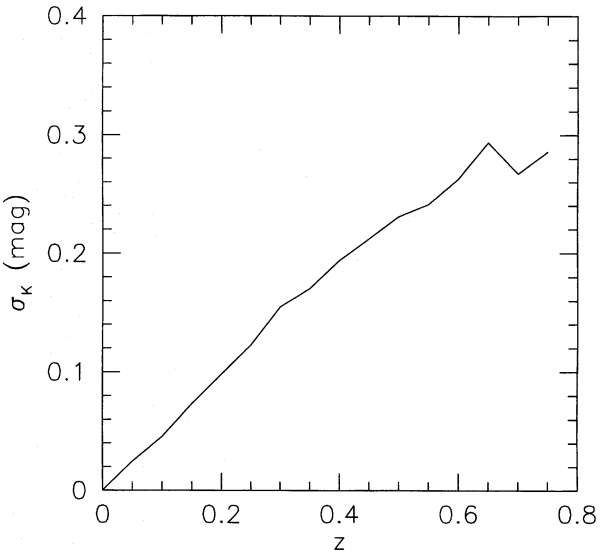

Figure 6. The rms error in the k-corrections as a function of redshift assuming 20 per cent of the galaxies are misclassed by ± 1 spectral class (see text for details).

are weighted by the numbers in each class to give the rms error plotted in Fig. 6. This error increases with z but is comparable to the photometric errors over the redshift range of the samples.

3.2 Luminosity function estimation

In our analyses we have used two related methods to estimate luminosity functions: the traditional $1/V_{max}$ method and a modified version of the step-wise maximum-likelihood method (SWML). The latter method was developed specifically for our survey and fulfils our requirement for extracting the LF within various redshift ranges from a number of catalogues lying within various magnitude limits. The $1/V_{max}$ method is more direct and provides an unbiased maximum-likelihood, minimum-variance estimate of the LF in the absence of clustering; SWML allows one to trade resolution in absolute magnitude for insensitivity to clustering. In the limit of small magnitude bins the two methods become identical. A full description of the modified SWML

method, and a comparison of the $1/V_{max}$ and SWML methods with other techniques for estimating LFs, is given in Paper II. Here, for simplicity, we present results based on the $1/V_{max}$ method. None of the conclusions in this paper is sensitive to the LF estimator used.

The $1/V_{max}$ method is the canonical direct estimator of the LF, first introduced by Schmidt (1968) for the study of quasar evolution (see also Felten 1976). Avni & Bahcall (1980) showed how to combine more than one sample in a $1/V_{max}$ analysis, and Eales (1993) extended the method to construct the LF as a function of redshift. The method works as follows.

Suppose we have N galaxies, and for each galaxy i we have measured its apparent magnitude m_i and its redshift z_i. These galaxies were obtained in M samples, and sample j covers an apparent-magnitude range $m_{1j} \le m \le m_{2j}$ and an area (solid angle) of sky ω_j (in steradians). It also has a sampling rate S_j (the fraction of galaxies in the given magnitude range and area that were observed) and a completeness C_j (the fraction of the observed galaxies for which redshifts were obtained). Any *known* dependence of the sampling rate or completeness on apparent magnitude, redshift or spectral type can be removed by appropriate weighting.

The LF (number of galaxies per unit comoving volume per unit magnitude) in the absolute-magnitude range $M_1 \le M \le M_2$ and redshift range $z_1 \le z \le z_2$ can then be estimated as

$$\frac{\int_{M_1}^{M_2}\int_{z_1}^{z_2}\phi(M, z)\,\mathrm{d}z\,\mathrm{d}M}{(M_2-M_1)(z_2-z_1)} = (M_2-M_1)^{-1}\sum_{\{i:\,M_1\le M_i\le M_2\}} 1/V_i, \qquad (1)$$

where the sum is over galaxies in the given absolute-magnitude range and V_i is the toal accessible volume of galaxy i. This volume is

$$V_i = \sum_{j=1}^{M} V_{ij}, \qquad (2)$$

where

$$V_{ij} = \Omega_j \int_{z_{\min}^{ij}}^{z_{\max}^{ij}} \frac{\mathrm{d}V}{\mathrm{d}z}\,\mathrm{d}z \qquad (3)$$

is the accessible volume of the galaxy i in sample j and $\Omega_j = \omega_j S_j C_j$ is the effective area in steradians of this sample. In this way we treat the M samples as a single coherent sample (following Avni & Bahcall 1980). The integral is over the comoving volume element (see below), and the limits are the lowest and highest redshifts at which galaxy i remains both within sample j's magnitude range $m_{1j} \le m \le m_{2j}$ and within the redshift range $z_1 \le z \le z_2$. If $z(M, c, m)$ is the redshift at which a galaxy of absolute magnitude M and spectral class c has an apparent magnitude m, then

$$z_{\min}^{ij} = \max\,[z_1, z(M_i, c_i, m_{1j})] \qquad (4)$$

and

$$z_{\max}^{ij} = \min\,[z_2, z(M_i, c_i, m_{2j})]. \qquad (5)$$

For completeness, we note that the absolute and apparent magnitudes of galaxy i are related by

$$M_i = m_i - 5\log d_L(z) - K(z, c_i) - A_i - 25, \qquad (6)$$

where A_i is the Galactic absorption in the direction of the galaxy (which we assume to be negligible throughout our analysis), $K(z, c_i)$ is its k-correction, and $d_L(z)$ is its luminosity distance in Mpc, given by

$$d_L(z) = \frac{cz}{H_0}\left[\frac{1+z+(1+2q_0z)^{1/2}}{1+q_0z+(1+2q_0z)^{1/2}}\right]. \qquad (7)$$

The volume element (in Mpc^3) corresponding to a solid angle of 1 sr and a thickness of dz at redshift z is

$$\frac{\mathrm{d}V}{\mathrm{d}z} = \frac{c}{H_0}\frac{d_L^2}{(1+z)^3(1+2q_0z)^{1/2}}. \qquad (8)$$

As shown by Felten (1976), the $1/V_{max}$ method is an unbiased, maximum-likelihood, minimum-variance estimator of the LF. However, clustering in the galaxy sample causes the $1/V_{max}$ estimator to produce spurious 'features' due to the assumption that the galaxy number density is everywhere constant (apart from a possible evolutionary variation with redshift). Thus a cluster at low redshift will be misinterpreted as an excess of intrinsically faint galaxies, while a cluster at high redshift will produce a spurious excess of luminous galaxies.

The uncertainties in the luminosity functions derived by the $1/V_{max}$ method can be obtained either using the approximate formula given by Felten (1976) or (as we have done here) by using standard bootstrap error estimation techniques. Note that we have not applied any corrections to our LFs for the photometric errors in our magnitudes. This is because (i) these corrections would be small, since the rms photometric errors are typically 0.1–0.2 mag, which is much smaller than the 0.5-mag bins we use for computing the LFs, and (ii) because uncertainties in the k-corrections are at least as large. We consider the effects of the latter in more detail below.

4 RESULTS

The distribution of absolute magnitude with redshift for the entire survey is shown in Fig. 7. Although it is not straightforward to interpret because of the various samplings, solid angles and magnitude limits of each subsurvey, and the effects of k-corrections on the relative numbers of different galaxy types, two important results (which we establish rigorously below) are already apparent. First, there appears to be a dearth of sources at the faint end of the LF locally, notwithstanding the very faint apparent-magnitude limits now probed by LDSS-1 and LDSS-2. This suggests that there is no significant population of low-luminosity sources (see the discussion by Glazebrook et al. 1995a). Secondly, considering those sources with strong [O II] emission, we note that both the abundance and mean luminosity of these star-forming galaxies appear to increase with redshift. In this section we examine what our combined survey can tell us about (i) the local LF, (ii) the evolution of the LF with

redshift, and (iii) the relative evolution of the star-forming galaxies compared with that of the entire sample.

4.1 The local luminosity function

There has been considerable debate on the question of whether the faint-end slope of the local LF has been underestimated. The motivation arises partly from theoretical expectations based on hierarchical cosmologies, where the required growth of structure can be seeded by dark matter haloes but only with an associated steep mass spectrum, corresponding to $\alpha \approx -1.3$ to -1.5 (Kauffmann et al. 1994). Elaborate mechanisms are required to circumvent this problem (Cen & Ostriker 1994).

Recent LF estimates (Efstathiou et al. 1988; Loveday et al. 1992; Marzke, Huchra & Geller 1994) consistently indicate a Schechter slope for all galaxies of $\alpha \simeq -1.1$ down to $M_B = -17 + 5 \log h$. This is in marked contrast to the LF computed for the nearby Virgo cluster (Binggeli, Sandage & Tammann 1988), and so the question has been raised whether the local field LF determinations have missed an abundant population of low-luminosity sources (see McGaugh 1994 and references therein). In their analysis of the CfA redshift survey, Marzke et al. (1994) claim the first evidence for a possible upturn fainter than $M_{\rm Zwicky} = -16 + 5 \log h$. Specifically, they observe three times as many low-luminosity objects in this category as would be expected from an extrapolation of the $\alpha = -1.1$ Schechter function fitted at higher luminosities. We believe that the uncertainties are still too great for Marzke et al.'s result to be considered definitive. A scale error in the photometric scale of the Zwicky catalogue could significantly reduce the excess, and the volume sampled at these absolute magnitudes is very small. Indeed, the effect is greatest in the northern cap, where Virgo galaxies inevitably contaminate the supposed field sample.

It is important here to distinguish between two distinct uncertainties in the local LF whose effects are often confused. First, as described above, the faint-end slope remains uncertain and a steep slope cannot formally be excluded from current data fainter than $M_B = -16$. This uncertainty is largely a consequence of the small volumes probed for galaxies with $M_B > -16$ by all extant surveys. In the combined CfA redshift survey of 10 620 galaxies over 2.8 steradians in both hemispheres to $M_{\rm Zwicky} = 15.5$, although 293 galaxies were found with $M_{\rm Zwicky} > -16$, they sample a volume contained within only 10–20 Mpc, which is unlikely to be representative. In the deeper Stromlo–APM 1:20 survey of 1769 galaxies over 4300 deg^2 to $b_{\rm J} = 17.15$, the depth is clearly greater, but the number fainter than $M_B \simeq -16$ is only 49. Notwithstanding these uncertainties, a steeper local LF would greatly increase the observed number of apparently faint galaxies, as intrinsically faint sources contribute a Euclidean number-count slope (Kron 1980; Phillips & Driver 1995). As discussed by Broadhurst et al. (1988), however, a very significant contribution of low-luminosity galaxies at $b_{\rm J} > 21$ would distort the field redshift distribution to lower values than observed. Clearly only more extensive surveys beyond $B = 17$, such as that discussed here, can resolve this issue definitively.

A second, and independent, uncertainty has been pointed out by many workers (e.g., Ferguson & McGaugh 1995), namely that many field surveys may miss altogether a population of low-surface-brightness galaxies (LSBGs) by virtue of selection effects inherent in standard image detection algorithms (Disney & Phillipps 1985; Davies, Disney & Phillipps 1989). As an undetected population, their location in the LF is a matter of conjecture. Most direct searches for LSBGs have found relatively few compared with the numbers of galaxies of normal surface brightness (Dalcanton 1994; Roukema & Peterson 1995). However, Schwartzenberg et al. (1995) have recently claimed to find 10 times as many LSBGs as normal galaxies brighter than $0.1L^*$. This

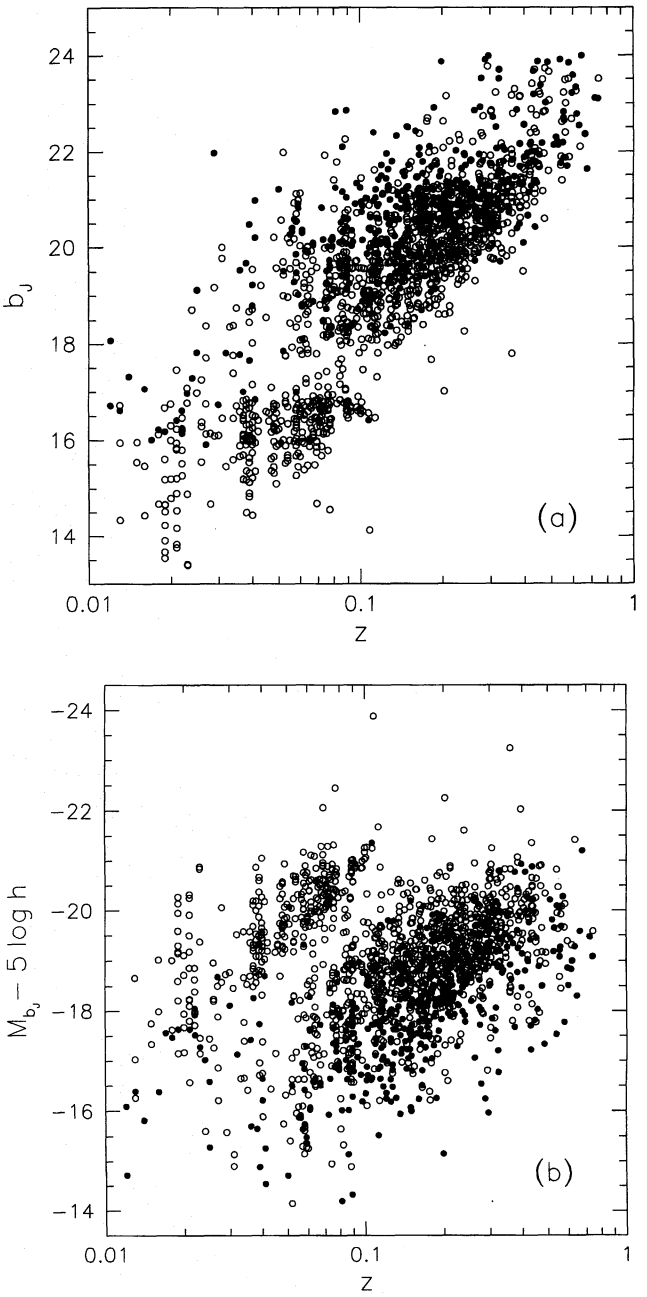

Figure 7. The survey data: (a) apparent-magnitude–redshift distribution, and (b) absolute-magnitude–redshift distribution. Galaxies with strong [O II] emission (those with restframe equivalent widths $W_\lambda \geq 20$ Å) are shown as filled circles.

claim requires further investigation, as it depends critically on indirect estimates for the redshifts of the objects involved.

Although one might assume that LSBGs lie predominantly at the faint end of the LF, thereby being relevant to the problem discussed above, this need not necessarily be the case. Indeed, some of the LSBGs so far identified are fairly luminous (Bothun, Impey & Malin 1989). If the surveys conducted at faint apparent magnitude systematically probed to lower-surface-brightness limits, they might reveal a higher volume density of galaxies over a range of luminosities, and hence more faint galaxies. In the rather unlikely case of similar LFs for the high- and low-surface-brightness populations, the hypothesis could be tested with surface-brightness profiles at various redshifts and magnitudes. Broadly speaking, one would expect to uncover more LSBGs at fainter limits.

The most straightforward argument *against* the theory that the faint galaxy population is dominated by LSBGs comes from recent ground- and space-based observations with sufficient resolution to determine the sizes of faint galaxies. Colless et al. (1994) found that the size–luminosity relation for a sample of 26 $b_J \approx 22$ galaxies drawn from the LDSS-1 survey, with redshifts up to $z \approx 0.7$, was entirely consistent with that of normal low-redshift spirals. Likewise, preliminary *Hubble Space Telescope* studies of galaxies to $I \approx 21$ (Mutz et al. 1994; Phillips et al. 1995) also show a stable size–luminosity relation and no excess of LSBGs.

Fig. 8 shows the local ($z < 0.1$) LFs derived from the DARS survey and from the combined AF-bright and AF-faint surveys (hereafter Autofib). The solid and short-dashed curves are the Schechter function fits to the Stromlo–APM survey by Loveday et al. (1992) and to the DARS survey by Efstathiou et al. (1988), respectively. The parameters of these fits are $M_{b_J} = -19.50$, $\alpha = -0.97$, $\phi^* = 0.014\ h^3$ Mpc^{-3} for Stromlo–APM and $M_{b_J} = -19.56$, $\alpha = -1.04$, $\phi^* = 0.008\ h^3$ Mpc^{-3} for DARS. The fits apply to the range $-22 \le M_{b_J} \le -17$; the dotted curves show the extrapolations to fainter magnitudes. The long-dashed curve is the Schechter function fit to the Autofib survey LF over the range $-20 \le M_{b_J} \le -14.5$, and has parameters $M_{b_J} = -19.20^{+0.29}_{-0.34}$, $\alpha = -1.09^{+0.10}_{-0.09}$, $\phi^* = 0.026^{+0.08}_{-0.08}\ h^3$ Mpc^{-3} ($\chi^2 = 11.6$ for 10 degrees of freedom).

The DARS and Stromlo–APM LFs agree at the bright and faint ends, but DARS has a deficit of galaxies with $-20 < M_{b_J} < -18$. This deficit leads to the two times lower normalization and slightly steeper faint-end slope in the Schechter fit to DARS. The low normalization of the DARS LF was noted by Efstathiou et al. (1988) in comparing the DARS counts with those of deeper photometric surveys; they claimed it was marginally consistent with the effects of clustering if uncertainties in the selection function were also taken into account.

The Autofib $z < 0.1$ LF is significantly higher than the Stromlo–APM LF everywhere fainter than $M_{b_J} = -19.5$; the LF is not well-defined brighter than this, where it is determined from only 17 galaxies. The faint end is again flat at least as faint as $M_{b_J} = -16$, but has a normalization that is about a factor of 2.5 higher than that of Stromlo–APM or DARS.

How can one interpret this change in the normalization between the DARS/Stromlo–APM LF and the Autofib LF?

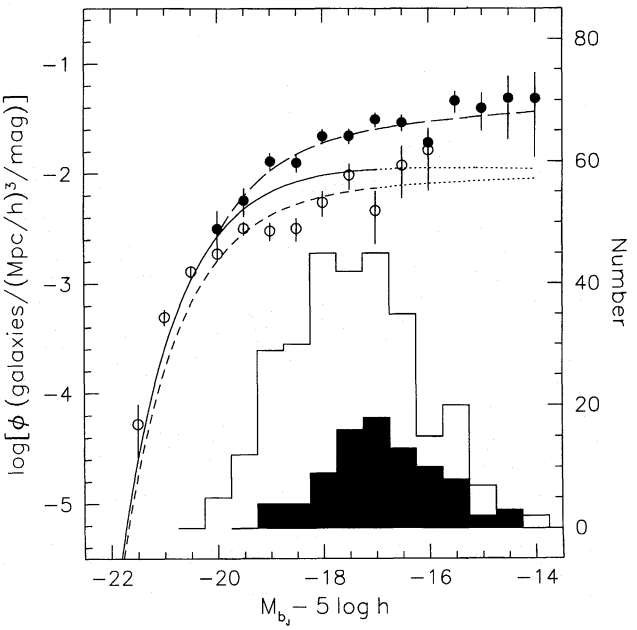

Figure 8. The local ($z < 0.1$) luminosity functions from the DARS survey (open circles) and combined surveys excluding DARS (filled circles). The solid curve is the Loveday et al. (1992) fit to the Stromlo–APM survey LF and the short-dashed curve is the Efstathiou et al. (1988) fit to the DARS LF (the dotted curves are the extrapolations of these fits from $M_{b_J} = -17$ to -14.5). The fit to the combined LF (excluding DARS) is shown as the long-dashed curve; the open histogram shows the absolute magnitudes of the galaxies contributing to this LF, while the shaded histogram shows the distribution of galaxies with $W_\lambda[\mathrm{O\,II}] > 20$ Å.

If it is due to evolution it is remarkably rapid: the galaxies at, say, $M_{b_J} = -17$ in the $b_J < 17$ surveys are at $z < 0.02$ while galaxies of the same luminosity in the Autofib surveys are close to the redshift limit imposed on this 'local' LF (i.e. $z = 0.1$), corresponding to a look-back time of only $0.9\ h^{-1}$ Gyr. An alternative explanation is some sort of measurement error in the bright or faint survey magnitudes, including residual isophotal effects associated with the fainter surface-brightness thresholds associated with the deeper survey data as advocated by Metcalfe, Fong & Shanks (1995b). This explanation also poses difficulties since a zero-point offset between the various surveys produces a horizontal rather than vertical shift in the LFs, while a magnitude scale error would produce a change in the faint-end slope.

The higher normalization in the observed local LF for surveys at fainter magnitude limits is the direct counterpart to the well-known observation that the number counts at $b_J < 19$ are much steeper than is predicted by a model with a non-evolving LF with a flat faint end. The solution to this puzzle is unclear, but one suggested resolution can be ruled out: the steep counts are *not* due to a non-evolving LF with a steep faint end (at least, not down to $M_{b_J} = -16$). Such a conclusion might be incorrectly drawn if one simply combined two surveys with different magnitude limits on the assumption that the LF does not change: combining the DARS and Autofib surveys to produce an overall $z < 0.1$ LF results in a misleadingly steep faint-end slope of $\alpha = -1.3$, despite the fact that each survey has $\alpha = -1.0$ because the

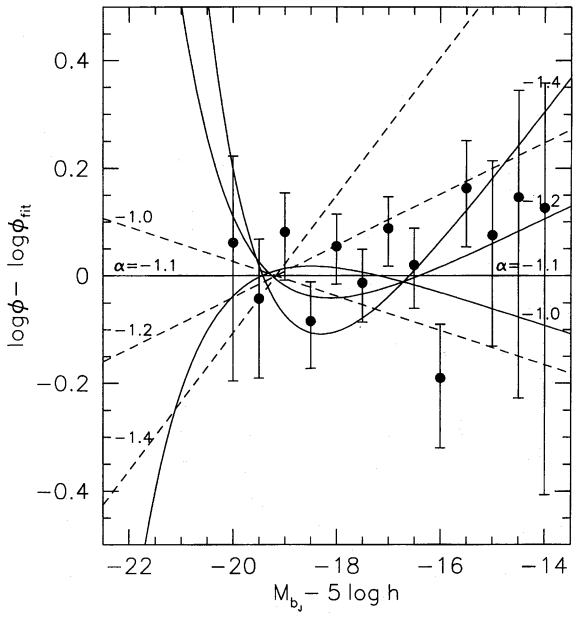

Figure 9. The slope of the faint end of the local LF. The points with error bars show the logarithmic differences between the observed local LF from the combined surveys (excluding DARS) and the best-fitting Schechter function ($M^* = -19.17$, $\alpha = -1.08$, $\phi^* = 0.027$). The various curves are the logarithmic differences between various alternative fits to the LF and this overall best fit. The solid curves are for the best-fitting Schechter functions with α fixed at -1.0, -1.2 and -1.4 (but M^* and ϕ^* allowed to vary); the dashed curves are for Schechter functions with the *same* M^* and ϕ^* as the overall $\alpha = -1.1$ best fit, but with α set to -1.0, -1.2 and -1.4.

bright end of such a combined LF is dominated by the low-normalization DARS LF while the faint end is dominated by the high-normalization Autofib LF. These arguments suggest the DARS sample may be unrepresentative, and thus we will exclude it in our further analyses.

Evidence for a higher normalization than that originally suggested by DARS has also come from independent *I*-band redshift surveys (Lilly et al. 1995), morphological-based counts obtained with the *Hubble Space Telescope* (Glazebrook et al. 1995c) and from LFs estimated from galaxies identified on the basis of their Mg II absorption lines in distant unrelated QSO spectra (Steidel, Dickinson & Persson 1994).

A further significant development from the Autofib survey, however, is that we can comment on the nature of the LF fainter than $M_{b_J} = -16$ more reliably than previous workers. This arises from two specific features of the survey. First, by probing fainter limits we survey deeper and more representative volumes. For example, at $M_{b_J} = -14$, galaxies can be located across all fields of the Autofib survey in a total effective volume of 2600 Mpc^3, 3.7 times larger than that appropriate for Marzke et al.'s (1994) CfA survey. Significantly, for the bulk of our survey reaching to $b_J \simeq 22$, such dwarfs would be seen to 160 h^{-1} Mpc (compared to only 8 Mpc in CfA), indicating much more representative volumes when the large number of independent pencil beams spanning the southern sky is taken into consideration (Section 2.1). Secondly, the faint end of the local LF is probed most effectively from the $b_J > 21$ samples selected from deep 4-m plates and ancilliary CCD data. This material was thresholded at a low-surface-brightness limit of approximately $\mu_{b_J} = 26.5$ mag arcsec^{-2} (Jones et al. 1991), which would guarantee detection of LSB galaxies of the kind proposed.

Since the samples are still small, the simplest way to proceed is to address the hypothesis that there is an upturn in the LF fainter than $M_B = -16 + 5 \log h$, as proposed by Marzke et al. (1994). Fig. 9 shows the ratio of the number of galaxies found in the survey at various luminosities (and its formal uncertainty) to that expected for the Schechter function given above (fitted over the brighter luminosity range down to $M_B = -16$). To test the sensitivity to α we have arbitrarily adjusted its value while keeping M_B^* and ϕ^* fixed. We also examined the case where M_B^* and ϕ^* are allowed to take their best-fitting values. In both cases, we find no evidence for an upturn of the faint end of the LF as claimed by Marzke et al. (1994), and a distinctly different behaviour to that identified by Binggeli et al. (1988). The steepest local LF slope consistent with our data has $\alpha \simeq -1.2$.

A related question is whether there is any difference between the properties of the intrinsically faint and luminous galaxies, such as might be expected if strong selection effects were limiting the detection of the low-luminosity sources. In the *cluster* samples, Binggeli et al. claim that the bulk of the low-luminosity galaxies are red compact dEs and blue dIrrs. Fig. 8 shows that virtually all of the sources fainter than $M_{b_J} \approx -17$ are strong star-forming galaxies with [O II] equivalent widths $W_\lambda > 20$ Å. Spectroscopically, these are virtually all classified as late-type systems similar to the Virgo dIrrs; no compact red sources are found.

Returning finally to the question of selection biases, it is important to recognize that the surveys most sensitive to the faint end of the local LF are those beyond $B > 21$, including those performed with LDSS-1 and LDSS-2 which address *all* sources, regardless of star/galaxy appearance. Thus compact extragalactic sources would not be missed in these surveys (Colless et al. 1991, 1993).

In summary, we have direct evidence that the absolute scale of the local LF is underestimated by brighter surveys, but, significantly, there is *no* evidence for a steeper faint-end slope at low redshift in any of the various data sets.

4.2 Evolution of the luminosity function

Broadhurst et al. (1988) proposed that the redshift distribution of their $b_J = 20$–21.5 survey might be reconciled with the excess number seen if the LF had a steeper faint-end slope in the past (see their fig. 9). At what is now a fairly modest magnitude limit, their conclusion was affected by the uncertainty in the absolute normalization of the LF. An upward shift of a factor of 1.5–2 in ϕ^* might remove the need for evolution in the BES data. At the fainter limits probed by LDSS-1 (Colless et al. 1990, 1993) and LDSS-2 (Glazebrook et al. 1995a), the uncertainties in normalization of the local LF are insufficient to explain the excess counts.

An additional argument used to justify evolution by the above-cited authors was that the *slope* of the counts, $\gamma = \mathrm{d} \log N / \mathrm{d}m$, is consistently steeper than the no-evolution prediction. Since, in the no-evolution prediction. Since, in

the no-evolution case, γ is independent of ϕ^*, this would appear to provide convincing evidence for some evolution. Unfortunately, this argument fails at some level because no convincing model based on the local LFs has yet reproduced γ in the bright, presumably non-evolving regime $15 < b_J < 20$ where a surprisingly steep count slope is also found (Maddox et al. 1990).

There are two issues that the Autofib survey can address. First, it can be used to establish directly whether there is a change in the LF shape with redshift, and, if so, for which class of sources the evolution is most apparent. Secondly, assuming the fields we have surveyed are representative of those used by Maddox et al. (1990), our survey might cast some light on the question of the true absolute normalization of the LF, which remains confused.

Fig. 10 shows the LFs derived from the $1/V_{max}$ method for the three broad redshift bins $0.02 < z < 0.15$, $0.15 < z < 0.35$ and $0.35 < z < 0.75$ corresponding to approximately equal time intervals of about 1.1 Gyr (for $H_0 = 100, q_0 = 0.5$). (Note that there are only four galaxies in the combined sample with $z > 0.75$). The size and depth of our survey enable us to derive reasonably accurate LFs in all three redshift ranges, although the highest-redshift LF only extends to $M_{b_J} \approx -18 + 5 \log h$ whereas the two lower-redshift bins extend to at least $M_{b_J} \approx -16 + 5 \log h$. The errors shown were obtained by bootstrap error analysis. In the case of the lowest-redshift bin, we have excluded the DARS sample following the discussion in Section 4.1. The figure clearly shows evidence for a steepening of the faint-end slope of the LF with increasing redshift, and perhaps an increase in the overall normalization. However, the trend is not completely clear as the LF at $M_{b_J} \simeq -19$ drops at intermediate redshifts and so evidently there are still fluctuations arising from the small sample size.

Formally, 1- and 2-sample χ^2 tests show that, in the region of overlap, the lowest-redshift LF in Fig. 10 does not differ in shape significantly from the local one (Fig. 8) since $P(>\xi^2) = 0.85$. The LFs in the higher-redshift bins differ from their lower-z adjacent bins, with $P(>\xi^2) = 0.219$ and 0.008, indicating that the bulk of the evolution sets in beyond $z \simeq 0.3$. Most of the apparent evolution inferred in earlier work within $0 < z < 0.3$ arose primarily because of the abnormally low LF normalization. The most significant result arises when we check whether the entire data set could be consistent with a non-evolving local LF. Considering the $-21.5 < M_{b_J} < -14.5$ LF with $0 < z < 0.75$ in six redshift bins, and maintaining a minimum bin count of five galaxies per absolute-magnitude interval, a χ^2 test rejects a non-evolving LF with a formal probability of $< 10^{-20}$.

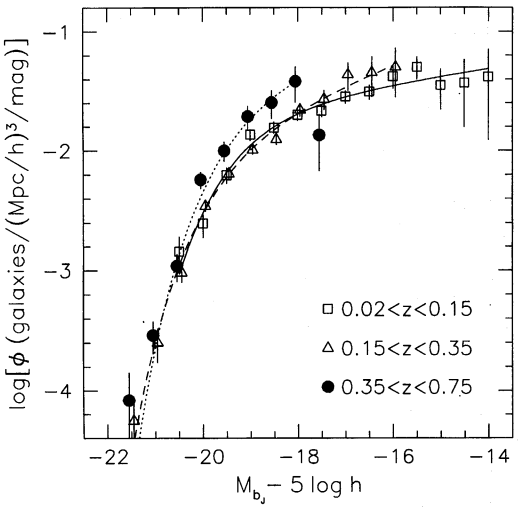

Figure 10. Evolution of the LF with redshift. The LF is shown for three redshift ranges, corresponding to approximately equal time intervals of about 1.1 Gyr.

The evolution appears to be stronger for galaxies fainter than L^*. The best-fitting Schechter functions for each redshift interval are listed in Table 2 and illustrated with their formal error bars in Fig. 11. Whereas the trend is not entirely continuous from one redshift range to another (as discussed above), it is important to note that the formal errors do not include any allowance for the possible effects of clustering. Given the small values of χ^2/ν and the discussion in Section 2.2., only a modest correction is expected. An increase in the error bars in Fig. 10 by $\sqrt{2}$ would be sufficient to explain the intermediate-redshift points at $M_{b_J} \simeq -19$ and would ensure continuity in the Schechter contours of Fig. 11. Although a larger sample is ideally required, it is clear from Figs 10 and 11 that the LF has evolved significantly over modest redshifts, and an important component of this evolution is in the faint-end slope. There is no convincing evidence for a systematic shift in $M^*_{b_J}$ over $z = 0$ to 0.75, whereas α steepens from -1.1 to -1.5.

Given the potential importance of this result, we need to examine whether it is stable to any procedural uncertainties in our analysis. We have already mentioned that the result is independent of the methods used to compute the LF from our data (see Paper II). In Section 3.1 we also discussed the small effects that incorrect *k*-corrections (arising from spectral misclassifications) might produce.

The application of the *magnitude*-dependent completeness correction for each survey in fact makes very little difference to the final LFs. The ratio of the LF with the correction to the LF without the correction in each redshift range is shown in Fig. 12. The changes are less than about 10 per cent expect where the number of galaxies contributing to the LF estimate is $\lesssim 10$.

We can place limits on the possible effects of *redshift*-dependent completeness by considering extreme cases where all the unidentified galaxies have either $z = 0.05$ or alternatively $z = 0.75$. Given our earlier discussion on redshift incompleteness, this must be considered highly unlikely but illustrates the robustness of our main result. If the incompleteness is assumed to be entirely local (Fig. 13a), the nearby LF steepens somewhat at the faint end although the evolutionary trends in Fig. 10 are still present. In the case where the incompleteness is assumed to be entirely at high redshifts (Fig. 13b), an unphysical discontinuity in normalization with redshift is produced, although, again, the evolution seen in Fig. 10 is maintained.

4.3 Faint star-forming galaxies

BES first suggested that the excess population might arise from a distinct population of star-forming galaxies. They noted an increasing number of strong [O II] emission-line

Table 2. Fitted parameters of the luminosity function with redshift.

z range	M^*	α	$\log\phi^*$	ϕ^*	χ^2 (ν)
$0.02<z<0.15$	-19.30 [-0.12,+0.15]	-1.16 [-0.05,+0.05]	-1.61 [-0.06,+0.06]	0.0245	8.62 (11)
$0.15<z<0.35$	-19.65 [-0.10,+0.12]	-1.41 [-0.07,+0.12]	-1.83 [-0.06,+0.08]	0.0148	8.68 (9)
$0.35<z<0.75$	-19.38 [-0.25,+0.27]	-1.45 [-0.18,+0.16]	-1.45 [-0.36,+0.26]	0.0355	4.57 (5)

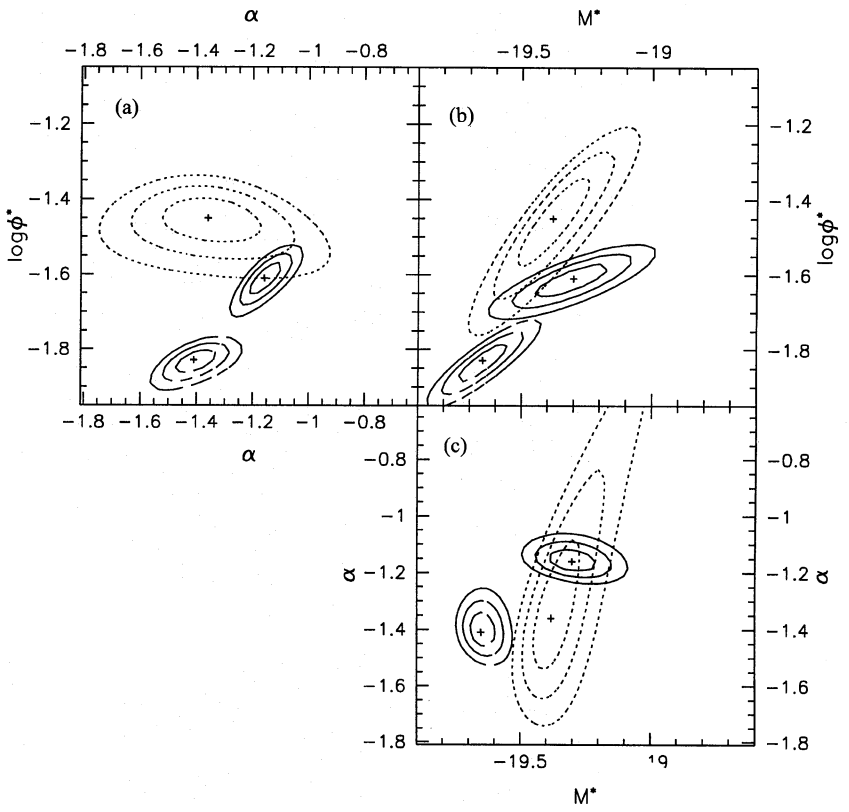

Figure 11. Error contours for the pairs of parameters (a) α and $\log\phi^*$, (b) M^* and $\log\phi^*$ and (c) M^* and α, fitted to the LFs obtained in the three redshift ranges $0.02<z<0.15$ (solid contours), $0.15<z<0.35$ (dashed contours) and $0.35<z<0.75$ (dotted contours). The contour levels shown are 1σ, 2σ and 3σ; the crosses indicate the best fits.

objects in their survey, and claimed that these might be sub-L^* galaxies rendered visible during a brief burst of star formation. By co-adding the spectra of several [O II]-strong galaxies, weak Balmer features were identified consistent with this hypothesis. Such a cycle would, however, imply that many more quiescent sources were present at fainter magnitudes beyond the limits of current surveys. Conceivably, many galaxies suffered these bursts in the past (with a rate increasing with redshift). Regardless of this, a large population of feeble sources has not yet been seen in local surveys, so these galaxies must somehow have disappeared from view. Broadhurst et al. (1992) later demonstrated that the star-forming sources, when separated according to their W_λ[O II], showed a remarkably steep count slope, whereas the remainder appeared to fit a no-evolution model. This would imply that rapid evolution takes place predominantly in the star-forming galaxies.

It is important to recognize that discontinuous star-formation events could readily transform a galaxy from being a member of the 'quiescent' population to one with strong [O II] or vice versa. At some level, it is misleading to consider spectrally classed populations as representing two independent components of the galaxy distribution. None the less, having established some form of evolution, it is important to find which kinds of sources are involved. A specific advantage of considering the [O II]-strong galaxies is the high redshift completeness assured by their emission spectra. This point was considered quantitatively by Colless et al. (1990) for samples limited by continuum signal-to-noise ratios. In view of previous claims for the central role of star formation in understanding the counts, an '[O II]-strong' subsample is likely to be a valuable data set for analysis.

Fig. 14 shows the change with redshift in the absolute-magnitude distribution and derived LFs for galaxies separated according to whether their W_λ[O II] exceeds or is less than 20 Å. Clearly there are major changes occurring for the star-forming galaxies. These sources show evolution qualitatively similar to, although stronger than, that observed for the whole population (cf. Table 3). Direct comparison of the high- and low-redshift LFs in Fig. 14a shows that the space density of star-forming galaxies has decreased at all

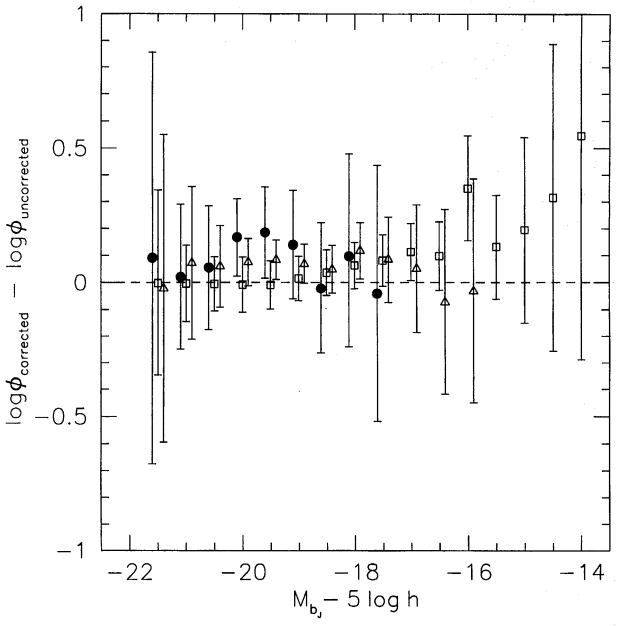

Figure 12. Logarithmic difference between the completeness-corrected and uncorrected LFs in the three redshift ranges shown in Fig. 10 (with the same symbols for each range).

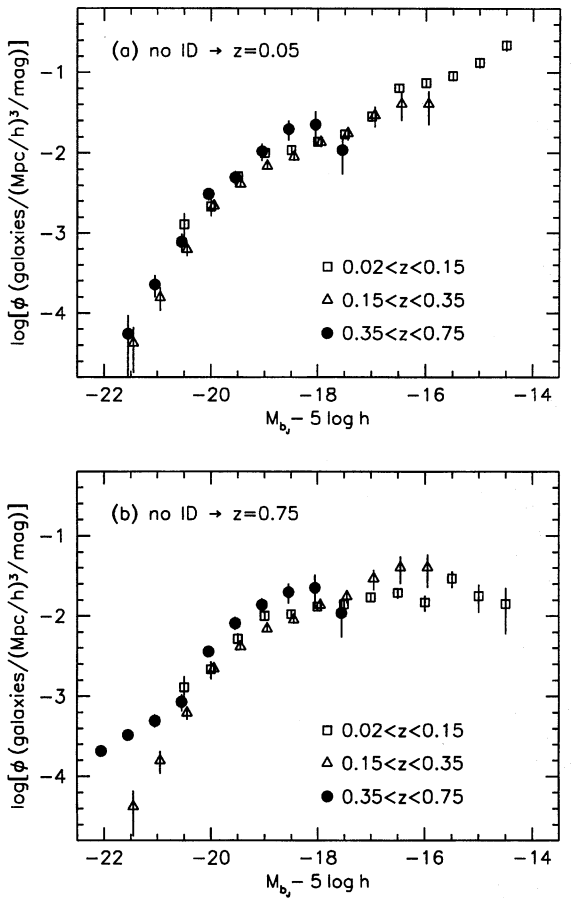

Figure 13. The LFs in three redshift ranges as in Fig. 10, but assuming that all the unidentified objects have (a) $z=0.05$ or (b) $z=0.75$, and that therefore the sample is 100 per cent complete.

luminosities by almost a factor of 2 between $z\approx0.4$ and $z\approx0.15$. This decline corresponds to an overall fading of the star-forming population of 0.5 mag over this redshift range.

The rapid evolution in the LF of the star-forming galaxies is consistent with a conclusion derived by Lilly et al. (1995) from from the *I*-band-selected CFRS survey. Those workers claim substantial brightening with redshift for *I*-selected galaxies whose rest-frame colours are bluer than Sbc type. In Paper II we address the question of evolution as a function of spectral class more rigorously. However, we note that Lilly et al.'s fig. 3(b) is quite similar to our Fig. 14, which is particularly encouraging considering the different selection criteria and methods used by the two groups.

It should be noted, however, that (i) by virtue of our *B*-selection we have a much greater sensitivity to this evolu-

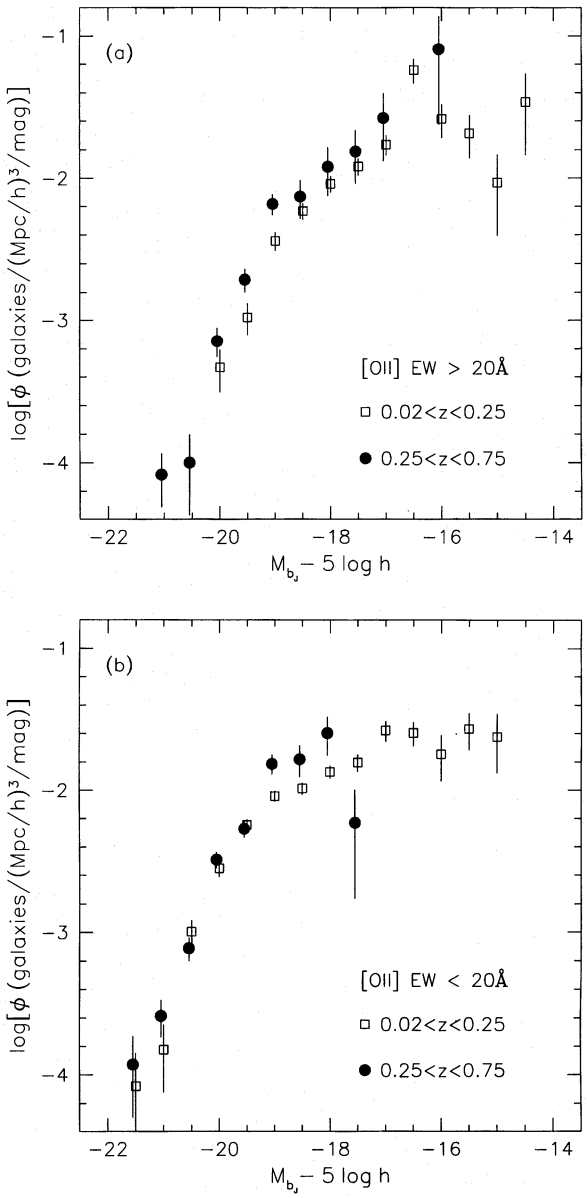

Figure 14. Luminosity functions at various redshifts for galaxies selected according to the equivalent width W_λ of the [O II] 3727-Å emission line.

Table 3. Luminosity function fits as a function of [O II]-equivalent width.

W_λ[O II] and z range	M^*	σ	log ϕ^*	ϕ^*	$\chi^2(\nu)$
$W_\lambda > 20$Å, $z < 0.25$	$-18.42\,[-0.14, +0.14]$	$-1.04\,[-0.08, +0.10]$	$-1.70\,[-0.06, +0.08]$	0.0200	22.53 (9)
$W_\lambda > 20$Å, $z > 0.25$	$-18.96\,[-0.30, +0.32]$	$-1.44\,[-0.26, +0.38]$	$-1.88\,[-0.24, +0.20]$	0.0132	8.82 (7)
$W_\lambda < 20$Å, $z < 0.25$	$-19.42\,[-0.12, +0.08]$	$-1.12\,[-0.06, +0.04]$	$-1.76\,[-0.06, +0.04]$	0.0174	9.59 (11)
$W_\lambda < 20$Å, $z > 0.25$	$-19.08\,[-0.18, +0.16]$	$-0.74\,[-0.22, +0.24]$	$-1.58\,[-0.08, +0.08]$	0.0263	20.84 (6)

tionary trend, and (ii) the wider range in apparent magnitude surveyed here provides a clearer estimate of the trends with luminosity at each redshift. In the CFRS survey, which spans only a limited apparent-magnitude range with its single magnitude-limited sample, it is very difficult to estimate the *shape* of the LF at any particular redshift. Conceivably, this is why Lilly et al. are unable, from their LF results, to reproduce the B-band counts (their fig. 8). On the other hand, the CFRS survey provides valuable information at higher redshifts (150 blue galaxies have $0.75 < z < 1.3$) by virtue of the reduced k-correction in the longer-wavelength band. The two surveys therefore complement each other remarkably well.

The question arises whether the [O II] sources are simply fading as a separate self-contained population? The answer is unclear because it is, necessarily, something of an arbitrary distinction as to whether a galaxy is put in the [O II]-strong or the quiescent sample. Certainly, if one starts with the high-redshift LF for the [O II]-strong galaxies in Fig. 14 applies a progressive luminosity-independent fading with redshift to the entire population, it is not possible to reconstruct Fig. 8 at $z=0$. Without some form of differential fading, there are too many star-forming galaxies at high z for the local representatives to be dimmed versions. No doubt the same dilemma would arise if one characterized the populations on the basis of colours as in Lilly et al. (1995). Neither colour nor spectral types is a particularly good classifier over a range in redshift since, when star formation falls below some threshold value, a galaxy can easily change from one category to another. One possible way forward may be to use *Hubble Space Telescope* morphology as the basic classifier, although it will be some time before such sizeable samples are available (Glazebrook et al. 1995c; Ellis 1996).

5 CONCLUSIONS

We summarize our principal conclusions as follows.

(i) We have completed a major new redshift survey of 1026 galaxies at intermediate magnitudes which, together with earlier published data secured by our team, allows us to construct a catalogue of over 1700 galaxy redshifts spanning a wide range in apparent magnitude from $b_J = 11.5$ to 24. The wide range in implied luminosity is a significant step forwards in determining directly the form of the luminosity function (LF) at various redshifts.

(ii) We confirm that the local LF has a Schechter faint-end slope with $\alpha \simeq -1.1$, as claimed by Efstathiou et al. (1988) and Loveday et al. (1992). A significantly steeper slope would lead to the detection of many more low-redshift galaxies than are observed in the faintest surveys. A careful analysis of the local LF derived from catalogues limited at different apparent magnitudes shows that the principal uncertainty in the local LF lies in its absolute normalization, not in its shape. We present convincing evidence for a LF normalization that is higher than that previously estimated, and this normalization is in agreement with other, indirect, estimates recently published.

(iii) Analysis of the galaxy LF as a function of redshift shows evidence for a steepening of the faint-end slope with increasing redshift, from Schechter values of $\alpha = -1.1$ locally to $\alpha = -1.5$ at redshift $z \simeq 0.5$. There is also a marked increase in the number of L^* galaxies over the look-back times sampled. We demonstrate the robustness of these results to various incompleteness effects inherent in the survey. These trends we have found provide a consistent explanation for the original puzzle of the excess galaxy counts and lack of evolution in the redshift distribution. The explanation confirms the original suggestion made by Broadhurst et al. (1988).

(iv) The evolution is consistent, to a reasonable approximation, with that arising primarily in the LF of strong star-forming galaxies categorized via the rest-frame equivalent width of [O II] 3727 Å. There has been a marked decline in the mean luminosity density of these star-forming sources since $z \simeq 0.5$, and it is this evolution that is responsible for the blue galaxy excess.

(v) In common with recent conclusions derived from counts categorized by *Hubble Space Telescope* morphologies, our LF studies have highlighted two galaxy populations which evolve in very different ways. Massive galaxies at the bright end of the LF show only marginal changes in their rest-frame B luminosities at recent times, whereas lower-mass galaxies suffer a rapidly declining star-formation rate.

ACKNOWLEDGMENTS

We thank Ian Parry, Ray Sharples, Peter Gray and staff at the AAT for their great efforts in making the Autofib instrument a reliable working system. We also thank PATT for their patience and support over many semesters. Keith Taylor and Jeremy Allington-Smith are thanked for their assistance with LDSS-1 and LDSS-2. We acknowledge useful discussions with Len Cowie, Olivier LeFevre, David Koo, Simon Lilly, Steve Maddox and Ron Marzke. RSE and KGB acknowledge financial support from PPARC. JSH thanks the Marshall Aid Commission. MMC acknowledges the assistance of the Australian Academy of Science/Royal Society exchange program.

REFERENCES

Avni Y., Bahcall J. N., 1980, ApJ, 235, 694
Binggeli B., Sandage A., Tammann G. A., 1988, ARA&A, 26,

509
Bothun G., Impey C. D., Malin D. F., 1989, ApJ, 341, 89
Broadhurst T. J., Ellis R. S., Shanks T., 1988, MNRAS, 235, 827 (BES)
Broadhurst T. J., Ellis R. S., Glazebrook K., 1992, Nat, 355, 55
Broadhurst T. J., Ellis R. S., Heyl J., Colless M., Glazebrook K., 1996, MNRAS, submitted
Cen R., Ostriker J. P., 1994, ApJ, 431, 451
Cole S. J., Aragón-Salamanca A., Frenk C. S., Navarro J. F., Zepf S. E., 1994, MNAS, 271, 744
Colless M. M., Ellis R. S., Taylor K., Hook R. N., 1990, MNRAS, 244, 408
Colless M. M., Ellis R. S., Taylor K. T., Shaw G., 1991, MNRAS, 253, 686
Colless M. M., Ellis R. S., Broadhurst T. J., Taylor K., Peterson B. A., 1993, MNRAS, 261, 19
Colless M. M., Schade D. J., Broadhurst T. J., Ellis R. S., 1994, MNRAS, 267, 1108
Cowie L. L., 1993, in Soifer T., ed., ASP Conf. Ser., Sky Surveys. Astron. Soc. Pac., San Francisco, p. 193
Cowie L. L., Songaila A., Hu E., 1991, Nature, 354, 460
Dalcanton J., 1994, ApJ, 415, L87
Davies J., 1990, MNRAS, 244, 8
Davies J., Disney M. J., Phillipps S., 1989, MNRAS, 239, 939
Disney M. J., Phillipps S., 1985, MNRAS, 216, 53
Eales S., 1993, ApJ, 404, 51
Efstathiou G., Ellis R. S., Peterson B. A., 1988, MNRAS, 232, 431
Ellis R. S., 1993, in Soifer T., ed., ASP Conf. Ser., Sky Surveys. Astron. Soc. Pac., San Francisco, p. 165
Ellis R. S., 1996, in Hut P., ed., Unsolved Problems in Astrophysics, Princeton Univ., in press
Felten J. E., 1976, ApJ, 207, 700
Ferguson H., McGaugh S., 1995, ApJ, 440, 470
Glazebrook K., Ellis R. S., Colless M., Broadhurst T. J., Allington-Smith J. R., Tanvir N. R., 1995a, MNRAS, 273, 157
Glazebrook K., Peacock J. A., Miller L. A., Collins C., 1995b, MNRAS, 275, 169
Glazebrook K., Ellis R. S., Santiago B., Griffiths R., 1995c, MNRAS, 275, L19
Heydon-Dumbleton N. H., Collins C. A., MacGillivray H. T., 1989, MNRAS, 238, 379
Heyl J. S., Ellis R. S., Colless M., Broadhurst T. J., 1996, MNRAS, submitted
Jones L. R., Shanks T., Fong R., Ellis R. S., Peterson B. A., 1991, MNRAS, 249, 481
Kauffmann G., Guiderdoni B., White S. D. M., 1994, MNRAS, 267, 981
Kennicutt R. C., 1992a, ApJS, 79, 255
Kennicutt R. C., 1992b, ApJ, 388, 410
King C. R., Ellis R. S., 1985, ApJ, 288, 456
Kirschner R. P., Oemler A., Schechter P., 1978, AJ, 83, 1549
Koo D. C., Kron R., 1992, ARA&A, 30, 613
Koo D. C., Gronwall C., Bruzual G. A., 1993, ApJ, 415, L21
Kron R., 1980, Vistas Astron., 26, 37
Lacey C., Guiderdoni B., Rocca-Volmerange B., Silk J., 1992, ApJ, 402, 15
Lilly S. J., 1993, ApJ, 411, 501
Lilly S. J., Cowie L. L., Gardner J. P., 1991, ApJ, 369, 79
Lilly S. J., Tresse L., Hammer F., Crampton D., LeFevre O., 1995, ApJ, 455, 108
Loveday J., Peterson B. A., Efstathiou G., Maddox S. J., 1992, ApJ, 390, 338
McGaugh S., 1994, Nat, 367, 538
Maddox S. J., Sutherland W. J., Efstathiou G. P., Loveday J., Peterson B. A., 1990, MNRAS, 273, 257
Marzke R., Huchra J. P., Geller M., 1994, ApJ, 428, 43
Metcalfe N., Shanks T., Fong R., Roche N., 1995a, MNRAS, 273, 257
Metcalfe N., Fong R., Shanks T., 1995b, MNRAS, 274, 769
Mutz S. B. et al., 1994, ApJ, 434, L55
Parry I. R., Sharples R. M., 1988, in Barden S. M., ed., PASP Conf. Ser. 3, Fiber Optics, San Francisco, p. 93
Pence W., 1976, ApJ, 188, 444
Peterson B. A., Ellis R. S., Bean A. J., Efstathiou G. P., Shanks T., Fong R., Zou Z-L., 1985, MNRAS, 221, 233
Phillipps S., Driver S., 1995, MNRAS, 274, 832
Phillips A C. et al., 1995, ApJ, 444, 21
Roukema B., Peterson B. A., 1995, A&A, 109, 511
Saunders W., Rowan-Robinson M., Lawrence A., Efstathiou G., Kaiser N., Ellis R. S., Frenk C. S., 1990, MNRAS, 242, 318
Schechter P., 1976, ApJ, 203, 297
Schmidt M., 1968, ApJ, 151, 393
Schwartzenberg J. M., Phillipps S., Smith R. M., Couch W. J., Boyle B. J., 1995, MNRAS, 275, 121
Steidel C., Dickinson M., Persson E., 1994, ApJ, 437, L75
Tritton K. P., Morton D. C., 1984, MNRAS, 209, 429